Modeling and Characterization of SiGe HBT Low-Frequency Noise Figures-of-Merit for RFIC Applications

Jin Tang, *Student Member, IEEE*, Guofu Niu, *Senior Member, IEEE*, Zhenrong Jin, *Student Member, IEEE*, John D. Cressler, *Fellow, IEEE*, Shiming Zhang, Alvin J. Joseph, *Member, IEEE*, and David L. Harame, *Senior Member, IEEE*

***Abstract*—We present the first systematic experimental and modeling results of noise corner frequency (f_C) and noise corner frequency to cutoff frequency ratio (f_C/f_T) for SiGe heterojunction bipolar transistors (HBTs) in a commercial SiGe RF technology. The f_C and f_C/f_T ratio are investigated as a function of operating collector current density, SiGe profile, breakdown voltage, and transistor geometry. We demonstrate that both the f_C and f_C/f_T ratio can be significantly reduced by careful SiGe profile optimization. A comparison of the f_C and f_C/f_T ratio for high breakdown and standard breakdown voltage devices is made. Geometrical scaling data show that the SiGe HBT with $A_E = 0.5 \times 2.5$ μm^2 has the lowest f_C and f_C/f_T ratio compared to other device geometries. An f_C reduction of nearly 50% can be achieved by choosing this device as the unit cell in RF integrated-circuit design.**

***Index Terms*—Breakdown voltage, corner frequency, cutoff frequency, device modeling, flicker noise, heterojunction bipolar transistor (HBT), low-frequency noise, phase noise, RF integrated circuit (RFIC), SiGe.**

I. Introduction

SiGe heterojunction bipolar transistor (HBT) technology has come of age as an important semiconductor technology for both wired and wireless telecommunications applications because of its superior analog and RF performance, together with its CMOS integration capability [1]. By employing bandgap engineering, SiGe HBTs outperform Si bipolar junction transistors (BJTs) in nearly every important performance metric and, in several areas, provide improved performance over the III–V HBTs. One of the areas in which SiGe HBTs exceed GaAs HBTs is in low $1/f$ noise corner frequency [2], thereby making them an excellent choice for low-noise amplifiers, oscillators [3], and power amplifiers.

The traditional figure-of-merit for low-frequency noise, the noise corner frequency (f_C), accounts for only $1/f$ noise. In circuit design, however, the speed of the transistors is also a critical design issue. Si BJTs typically have low f_C, but do not have sufficient gain to sustain oscillation at RF and microwave frequencies because of their limited f_T. GaAs HBTs have high f_T, but typically have high f_C and, hence, generate larger phase noise when used in oscillators. SiGe HBTs, however, provide f_T comparable to GaAs HBTs and lower f_C than Si BJTs, making them an attractive choice for ultra-low phase-noise oscillators [3]. A better figure-of-merit to characterize low-frequency noise for these applications is the f_C/f_T ratio [4], originally defined in [5], because it takes into account high-frequency response through f_T.

This paper presents modeling and experimental results of the low-frequency noise figures-of-merit f_C and f_C/f_T in a commercial SiGe RF technology. Low-frequency noise spectra and high-frequency s-parameters were measured, from which f_C and f_T are extracted. Four SiGe HBT wafers featuring different SiGe profile designs were used to examine the impact of SiGe profile shape on f_C and f_C/f_T . The profile comparison results are then used to derive a new figure-of-merit for SiGe profile design. Many wireless systems operate at frequencies below 50 GHz, the peak f_T achieved in this SiGe technology. The excess f_T can be traded for higher breakdown voltage to allow larger signal power, which reduces additive phase noise in voltage-controlled oscillators [6]. We will examine how the fabrication process modifications required for increasing breakdown voltage affects low-frequency noise, which then determines modulative phase noise in oscillators.

To facilitate optimum choice of biasing current in circuit design, f_C and f_T were measured across a wide range of operating current. One of the levers in RF integrated-circuit (RFIC) design is that the device size and layout can be used as design variables. Emitter length, for example, can be optimized for active noise matching in low-noise amplifier (LNA) design [7]. The same total device area required is typically obtained by parallel connection of small area unit cells. An array of SiGe HBT unit cells with different emitter areas are characterized over a wide range of biasing current to facilitate the optimum choice of device geometry, biasing current, and unit cell size that minimizes the low-frequency noise.

Manuscript received April 4, 2002. This work was supported by the National Science Foundation under Grant ECS-0 119 623 and Grant ECS-0112923, by the Semiconductor Research Corporation under Grant SRC 2001-NJ-937 and Grant 2000-HJ-769, by IBM under a Faculty Partnership Research Award, and by the Alabama Microelectronics Science and Technology Center.

J. Tang, G. Niu, and S. Zhang are with the Alabama Microelectronics Science and Technology Center, Electrical and Computer Engineering Department, Auburn University, Auburn, AL 36849 USA (e-mail: tangjin@eng.auburn.edu).

Z. Jin and J. D. Cressler were with the Alabama Microelectronics Science and Technology Center, Electrical and Computer Engineering Department, Auburn University, Auburn, AL 36849 USA. They are now with the School of Electrical and Computer Engineering, Georgia Institute of Technology, Atlanta, GA 30332-0250 USA.

A. J. Joseph and D. L. Harame are with IBM Microelectronics, Essex Junction, VT 05452 USA.

Digital Object Identifier 10.1109/TMTT.2002.804519

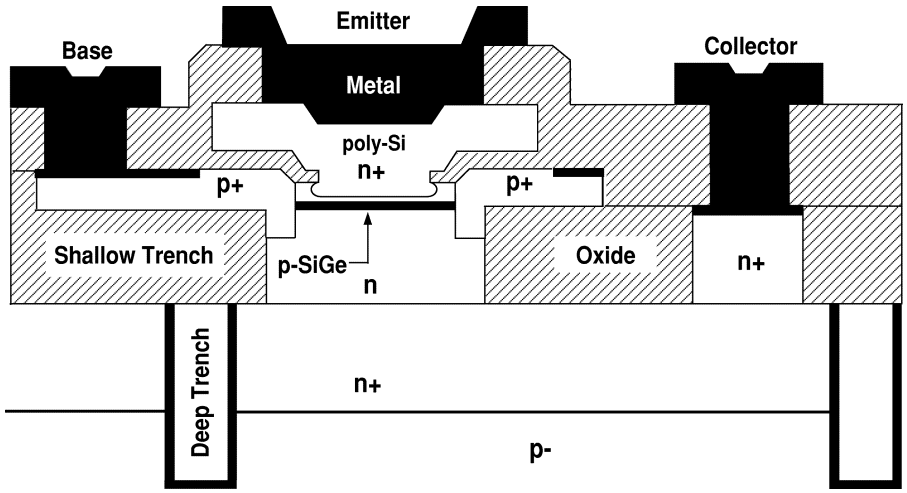

Fig. 1. Schematic cross section of the SiGe HBTs used in this study.

II. Device Technology

Fig. 1 shows a schematic cross section of the SiGe HBT used in this study. The SiGe HBT has a planar self-aligned structure with a conventional polyemitter contact, silicided extrinsic base, and deep- and shallow-trench isolation. The SiGe base was grown using the ultrahigh vacuum/chemical vapor deposition (UHV/CVD) technique. Devices of two different breakdown voltages were obtained on the same chip in the same fabrication flow by selective implantation during collector formation. The standard breakdown voltage (SBV) devices received both a deep and a shallow collector implant, and have a peak f_T of 50 GHz ($\mathrm{BV_{CEO}} = 3.3$ V). The high breakdown voltage (HBV) devices received only the deep collector implant, and have a peak f_T of 30 GHz ($\mathrm{BV_{CEO}} = 5.3$ V). Details of the fabrication process can be found in [8].

Four wafers with different SiGe profile designs were measured, including a 10% peak SiGe control, a 14% peak low-noise design ($LN1$), a 18% peak low-noise design ($LN2$), and an Si BJT comparison. Details of the SiGe profile design can be found in [9] and [10]. All of the wafers were fabricated in the same wafer lot under identical processing conditions. The SiGe films in all of the SiGe designs are unconditionally stable to defect generation. Compared to the SiGe control, the $LN1$ and $LN2$ designs have a higher Ge content and a larger Ge gradient in the neutral base to achieve higher β and higher f_T, but less Ge retrograding into the collector to keep the total Ge content within the thermal stability limit.

III. Low-Frequency Noise Figures-of-Merit

It has been experimentally established that the major $1/f$ noise source in these SiGe HBTs is the base current $1/f$ noise [2], [3]. The $1/f$ noise is proportional to I_B^{α} and inversely proportional to the emitter area A_E as follows:

$$S_{I_B} = \frac{K}{A_E} I_B^{\alpha} \frac{1}{f} \tag{1}$$

where K is a technology dependent constant, and $\alpha \approx 2$ for typical SiGe HBTs. K/A_E corresponds to the flicker noise constant K_F in SPICE. The noise corner frequency f_C is obtained by equating the $1/f$ noise S_{I_B} to the shot noise $2qI_B$ as follows:

$$f_C = \frac{KI_B}{2qA_E} = \frac{KJ_C}{2q\beta} \tag{2}$$

where $\alpha = 2$ is assumed for simplicity and insight, as detailed below, J_C is the collector current density, and β is the dc current gain.

Equation (2) suggests that f_C is proportional to J_C and K, and inversely proportional to β. This differs from that derived in [5]. The derivation of [5] showed that f_C is independent of biasing current density because $\alpha = 1$ was assumed according to mobility fluctuation. This, however, is not the case in our devices, which all show an α close to two.

The figure-of-merit for frequency response, cutoff frequency f_T, is related to J_C by

$$\frac{1}{2\pi f_T} \approx \tau_F + \frac{1}{g_m} C_t = \tau_F + \frac{V_t}{J_C} C_t \tag{3}$$

where τ_F is the forward transit time, $V_t = kT/q$ is the thermal voltage, $g_m = J_C/V_t$ is the transconductance per unit area, and C_t is the total junction depletion capacitance per unit area. Prior to f_T rolloff at high J_C, τ_F and C_t are constant in the typical J_C range of interest to RF circuits (0.1–1.5 mA/μm^2). The f_C/f_T ratio is obtained by combining (2) and (3) as follows:

$$\frac{f_C}{f_T} = K\frac{\pi}{q}\frac{J_C}{\beta}\left(\tau_F + V_t\frac{C_t}{J_C}\right) = \frac{K\pi}{\beta q}\left(\tau_F J_C + V_t C_t\right). \tag{4}$$

Thus, the model suggests a *linear* increase of the f_C/f_T ratio with operating collector current density J_C provided that β and τ_F are constant. This is in contrast to the prediction of a J_C independent f_C/f_T ratio in [5], which assumed $\alpha = 1$ ($\alpha \approx 2$ in our devices). At higher J_C, where f_T is larger, $\tau_F J_C \gg V_t C_t$ and $f_C/f_T \approx K\pi\tau_F J_C/\beta q$. Thus, the f_C/f_T ratio is determined by the $K\tau_F/\beta$ term at higher J_C. A smaller τ_F, higher β, and smaller K factor are desired to reduce f_C/f_T. A smaller f_C/f_T indicates better phase noise performance at higher frequencies.

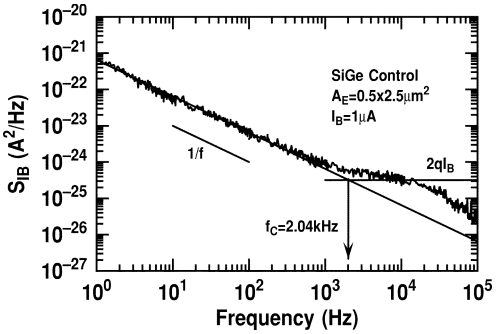

Fig. 2. Typical low-frequency noise spectrum of SiGe HBT used in this study ($A_E = 0.5 \times 2.5\ \mu\text{m}^2$, $I_B = 1\ \mu\text{A}$).

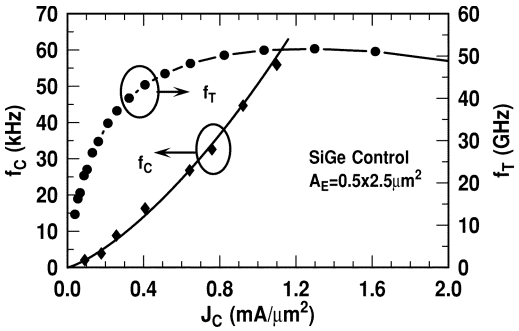

Fig. 3. Measured corner frequency f_C and cutoff frequency f_T as a function of J_C for the SBV SiGe control HBT ($A_E = 0.5 \times 2.5\ \mu\text{m}^2$).

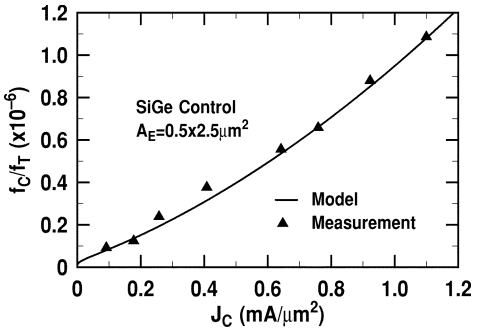

Fig. 4. Measured and modeled f_C/f_T ratio as a function of J_C for the SBV SiGe control HBT ($A_E = 0.5 \times 2.5\ \mu\text{m}^2$).

IV. Experimental Results

Low-frequency noise spectra and s-parameters were measured on both SBV and HBV devices for the SiGe control, the $LN1$ and $LN2$ low-noise SiGe designs, and the Si BJT comparison. Low-frequency noise was measured using an EG&G 5113 preamplifier and an HP3561A dynamic signal analyzer controlled by a Labview program. S-parameters were measured from 0.5 to 40 GHz using an HP8510C vector network analyzer, from which f_T was extracted. The forward transit time τ_F and the depletion capacitance per unit area C_t were determined from the intercept and slope of the linear extrapolation of the measured $1/f_T - 1/J_C$ data, respectively. In the low-frequency noise measurements, devices were biased at collector current densities from 0.1 to 1.5 mA/μm^2, the range of interest to RF circuits for the SBV devices.

Fig. 2 shows a typical low-frequency base current noise spectrum (S_{I_B}) for an SBV SiGe control HBT. The noise spectrum shows a clear $1/f$ component and the $2qI_B$ shot noise level. The corner frequency f_C is determined from the intersection of the $1/f$ component and the $2qI_B$ shot noise level. The rolloff above 10 kHz is due to the bandwidth limitation of the preamplifier used. The measured $S_{I_B} \times f$ product was plotted as a function of I_B, from which the SPICE $1/f$ noise constant K_F was extracted by assuming $\alpha = 2$. The obtained K_F is approximately proportional to $1/A_E$, leading to an emitter area independent K factor of $2.0 \times 10^{-9}\ \mu\text{m}^2$. The measured K factor is approximately the same for all of the SiGe designs.

A. Collector Operating Current Dependence

The measured and calculated f_C versus J_C are shown on the left y-axis of Fig. 3 for an SBV HBT on the SiGe control wafer. The measured f_T versus J_C dependence is shown on the right y-axis. The cutoff frequency f_T increases with J_C according to (3) prior to the f_T rolloff at high injection. The corner frequency f_C increases with J_C, as predicted by (2). The common practice of quoting corner frequency value without specifying biasing current and device geometry can be misleading because f_C strongly depends on biasing current density, as shown by the data in Fig. 3. The calculated f_C is in close agreement with measured data. The slight deviation from a linear increase is caused by the J_C dependence of β and the deviation of α from two. Fig. 4 shows the measured f_C/f_T ratio, together with modeling results calculated using (4). The modeling results agree well with the measured data. The f_C/f_T ratio increases with J_C, as predicted by (4). These results suggest that in order to reduce the f_C and f_C/f_T ratio, the smallest J_C that provides adequate f_T should be used.

B. High Breakdown Versus Low Breakdown

One of the most favorable properties of SiGe HBTs is the low $1/f$ corner frequency f_C, which makes them excellent choices for power amplifiers and oscillators [1]. In VCOs operating below the peak cutoff frequency of the HBV device (30 GHz), the HBV device is a better choice than the high f_T device. The HBV device has the natural advantage of operating with a larger signal power, thus reducing additive phase noise according to Leeson's theory [11].

A logical question is how the use of the HBV device affects the modulative phase noise up-converted from low-frequency noise. Fig. 5 compares the $S_{I_B} \times f$ product as a function of I_B for SBV and HBV devices on the SiGe control wafer. At the same I_B, the SBV and HBV devices show nearly the same $S_{I_B} \times f$ product. Due to their similar β, the two devices show nearly identical f_C at the same J_C, as shown in Fig. 6. Fig. 7 shows the measured and modeled f_C/f_T ratio versus J_C, together with measured f_T for both devices. At lower J_C, f_T is very close in the SBV and HBV devices. As J_C increases, f_T in the HBV devices decreases because of the enhanced Kirk effect due to the low collector doping. This f_T difference translates into an f_C/f_T difference. The f_C/f_T ratio is very close in the SBV and HBV devices before the f_T rolloff at high injection. The f_C/f_T ratio becomes higher in the HBV device after the f_T rolloff.

The similar low-injection $1/f$ noise behavior in the SBV and HBV devices indicates that the $1/f$ noise sources created by the

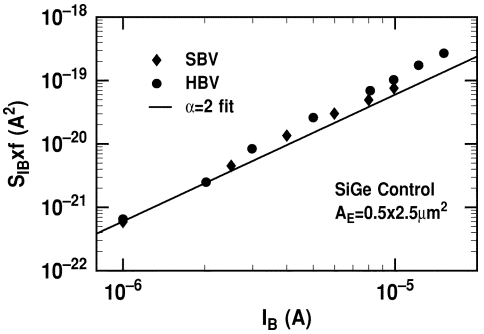

Fig. 5. Measured $S_{I_B} \times f$ product as a function of I_B for the SBV and HBV SiGe control HBTs ($A_E = 0.5 \times 2.5\ \mu\text{m}^2$).

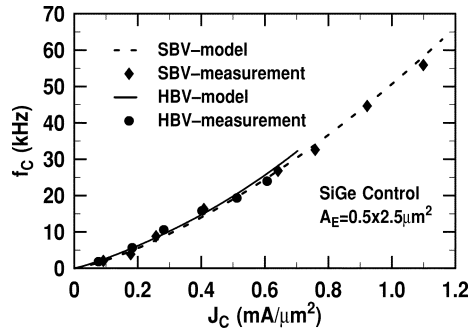

Fig. 6. Measured and modeled f_C as a function of J_C for the SBV and HBV SiGe control HBTs.

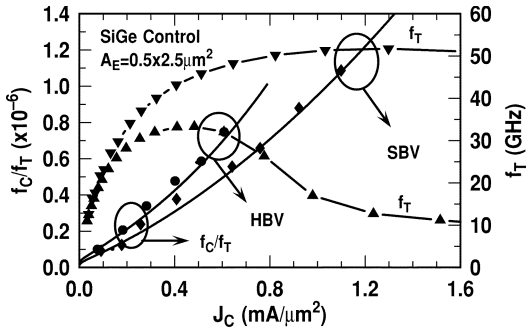

Fig. 7. Measured and modeled f_C/f_T ratio (left-hand side) and measured f_T (right-hand side) for the SBV and HBV SiGe control HBTs.

collector implantation through the SiGe base do not contribute significant $1/f$ noise. Since the up-conversion process is similar in the HBV and SBV devices, we expect the modulative phase noise in the HBV device to be as low as that in the high f_T SBV device for current densities lower than the peak f_T J_C.

C. SiGe Profile Dependence and Profile Design Implications

The two low-noise SiGe profiles, $LN1$ and $LN2$, were optimized to improve β, f_T, and $\text{NF}_{\min}$ without sacrificing SiGe film stability and peak f_T [9], [10]. Fig. 8 shows the measured f_T data for the SiGe control, the two low-noise HBTs, and the Si BJT comparison. All of the SiGe HBTs have much higher f_T than the Si BJT. $LN1$ and $LN2$ have a slightly higher f_T than the SiGe control. The measured $1/f$ noise K factor is nearly identical for all of the SiGe designs. We thus expect a significant reduction of f_C, as well as f_C/f_T in the two low-noise SiGe designs according to (2) and (4).

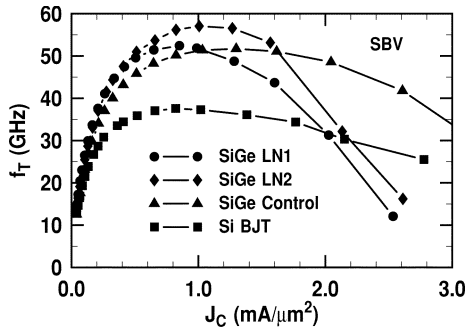

Fig. 8. Measured f_T as a function of J_C for the SBV Si BJT, SiGe control, and two low-noise HBTs.

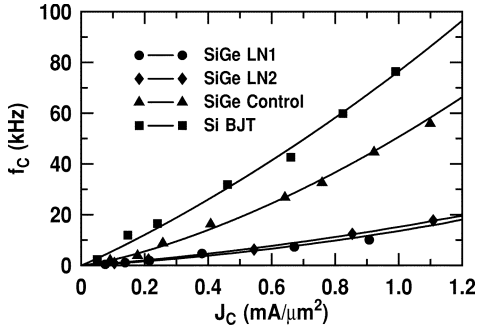

Fig. 9. Measured f_C as a function of J_C for the SBV Si BJT, SiGe control, and two low-noise HBTs.

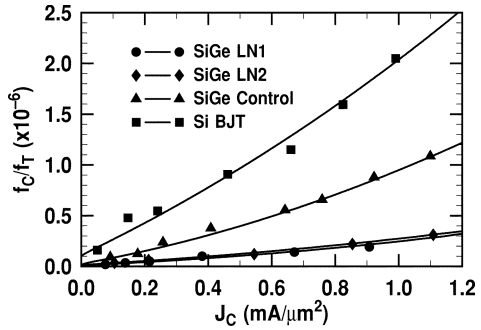

Fig. 10. Measured and modeled f_C/f_T ratio as a function of J_C for the SBV Si BJT, SiGe control, and two low-noise HBTs.

The measured f_C data shown in Fig. 9 confirms this expectation. The noise corner frequency f_C is indeed the lowest in $LN1$ and $LN2$, and highest in the Si BJT. The f_C/f_T ratio is the lowest in the two low-noise HBT designs because of the much lower f_C and slightly higher f_T, as shown in Fig. 10. For the same operating frequency, SiGe profiles optimized for high β, and high f_T should have better phase noise performance because of the lower f_C. To achieve the same RF gain, transistors with a higher f_T have the advantage to operate at a lower J_C, which further reduces f_C and phase noise.

The above results suggest that the τ_F/β ratio can be used as a figure-of-merit for SiGe profile optimization because f_C/f_T is proportional to $K\tau_F/\beta$ according to (4). The K factor is primarily determined by the emitter structure, and independent of the SiGe profile, as well as the collector doping profile, as evidenced by the experimental data. An SiGe profile producing the lowest τ_F/β ratio leads to the best f_C/f_T ratio, and should have the best phase noise performance at higher frequencies.

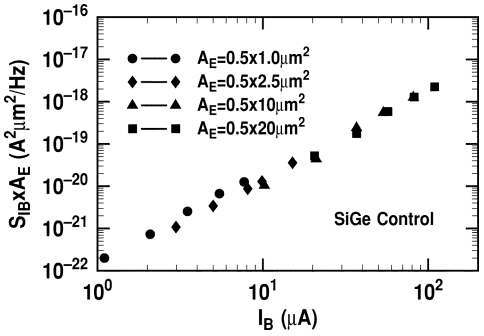

Fig. 11. Measured $S_{I_B} \times A_E$ versus J_C for SiGe control standard breakdown devices with four different emitter areas ($A_E = 0.5 \times 1.0\ \mu\text{m}^2$, $0.5 \times 2.5\ \mu\text{m}^2$, $0.5 \times 10\ \mu\text{m}^2$, and $0.5 \times 20\ \mu\text{m}^2$).

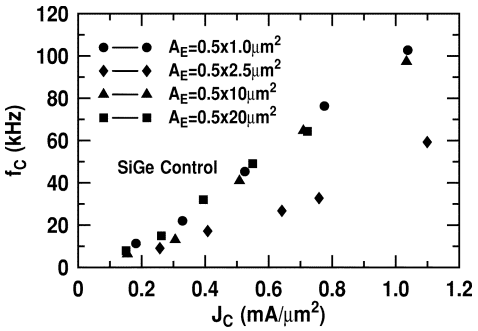

Fig. 12. Measured f_C versus J_C for SiGe control standard breakdown devices with four different emitter areas ($A_E = 0.5 \times 1.0\ \mu\text{m}^2$, $0.5 \times 2.5\ \mu\text{m}^2$, $0.5 \times 10\ \mu\text{m}^2$, and $0.5 \times 20\ \mu\text{m}^2$).

The modeled f_C and f_C/f_T ratio for the Si comparison, SiGe $LN1$, and SiGe $LN2$ were calculated according to (2) and (4), which were derived using $\alpha = 2$. The α for SiGe control (2.24), however, deviates from two. The deviation can be taken into account by using α as a model parameter in the derivation of f_C and f_C/f_T. The resulting equations are

$$f_C = \frac{KI_B^{\alpha-1}}{2qA_E} = \frac{KJ_C^{\alpha-1}}{2qA_E^{2-\alpha}\beta^{\alpha-1}} \tag{5}$$

$$\frac{f_C}{f_T} = \frac{K}{A_E^{2-\alpha}}\frac{\pi}{q}\frac{J_C^{\alpha-1}}{\beta^{\alpha-1}}\left(\tau_F + V_t\frac{C_t}{J_C}\right) = \frac{K\pi}{\beta^{\alpha-1}qA_E^{2-\alpha}}\left(\tau_F J_C^{\alpha-1} + V_t C_t J_C^{\alpha-2}\right). \tag{6}$$

The K factor is now defined using $S_{I_B} \times f = KI_B^{\alpha}/A_E$, and has dimensions of $A^{2-\alpha}\ \mu\text{m}^2$. These modified equations were used to calculate the modeling curve for SiGe control. The modification is necessary to achieve quantitative agreement with measurement for SiGe control. Equations (2) and (4), however, provide better insight and intuitive understanding of the biasing current density dependence because of simple functional forms.

D. Geometrical Scaling and Optimal Transistor Sizing

In RFIC design, the device geometry and layout are often used as design variables. The total emitter length required is often physically realized by connecting a number of small area unit cells in parallel. To investigate the low-frequency noise performance of unit cells with different emitter areas, measurements were made on the standard SiGe control wafer for the four device emitter areas: 1) $A_E = 0.5 \times 1.0\ \mu\text{m}^2$; 2) $A_E = 0.5 \times 2.5\ \mu\text{m}^2$; 3) $A_E = 0.5 \times 10\ \mu\text{m}^2$; and 4) and $A_E = 0.5 \times 20\ \mu\text{m}^2$.

Fig. 11 compares the $S_{I_B} \times A_E$ product as a function of the base current I_B for the four devices. SiGe control HBTs of different emitter sizes show the same base current noise and emitter area product $(S_{I_B} \times A_E)$ when biased at the same base current. Fig. 12 shows the noise corner frequency (f_C) versus collector current density (J_C) for different emitter areas. To our surprise, the $A_E = 0.5 \times 2.5\ \mu\text{m}^2$ device has the lowest f_C at the same J_C. First-order theory predicts the same f_C if β is assumed to be invariant among different emitter areas. This, however, is not the case in these devices, as shown by the measured β versus J_C data given in Fig. 13. The $A_E = 0.5 \times 2.5\ \mu\text{m}^2$ device has a higher β than the other three geometries. The higher β for this geometry is consistently observed on both the Si control wafer and the three SiGe HBT wafers, and is possibly due to the strain induced by the shallow trench isolation. K factors and J_C being the same, a higher β leads to a lower f_C because f_C is inversely proportional to current gain. On the other hand, for a given J_C, f_T is independent of geometry before high injection f_T rolloff [12]. The β difference among different geometries translates into an f_C/f_T difference. Under the same J_C, the $A_E = 0.5 \times 2.5\ \mu\text{m}^2$ HBT has the lowest f_C and f_C/f_T, therefore, it is an optimum unit cell choice for device layout. For instance, if the total effective emitter area required is $A_E = 0.5 \times 10\ \mu\text{m}^2$, a parallel combination of four $A_E = 0.5 \times 2.5\ \mu\text{m}^2$ HBTs should have a better low-frequency noise performance than ten $A_E = 0.5 \times 1.0\ \mu\text{m}^2$ HBTs in parallel, or one $A_E = 0.5 \times 10\ \mu\text{m}^2$ HBT. A corner frequency reduction of nearly 50% can be achieved by using an optimum unit cell size.

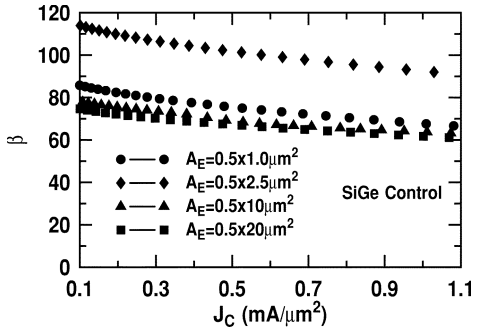

Fig. 13. Measured β versus J_C for SiGe control standard breakdown devices with four different emitter areas ($A_E = 0.5 \times 1.0\ \mu\text{m}^2$, $0.5 \times 2.5\ \mu\text{m}^2$, $0.5 \times 10\ \mu\text{m}^2$, and $0.5 \times 20\ \mu\text{m}^2$).

V. Conclusion

We have presented modeling and experimental results of corner frequency (f_C) and corner frequency to cutoff frequency ratio (f_C/f_T) in a commercial SiGe HBT technology. The corner frequency f_C is proportional to the collector current density J_C, and inversely proportional to β. The f_C/f_T ratio is proportional to the product of J_C, the forward transit time τ_F, the $1/f$ noise factor K, and is inversely proportional to β. The

HBV devices show nearly the same f_C and f_C/f_T ratio as the high f_T devices at lower J_C prior to the f_T rolloff. Measurements of devices featuring various SiGe profile designs show that both f_C and the f_C/f_T ratio can be significantly reduced by careful SiGe profile optimization without sacrificing SiGe film stability. The results also suggest that the τ_F/β ratio can be used as a $1/f$ noise figure-of-merit for SiGe profile and collector doping profile optimization in device design. The noise corner frequency was found to be device geometry dependent, and can be reduced by as high as 50% when the $0.5 \times 2.5\ \mu\text{m}^2$ HBT is used as the unit cell in RFIC design.

ACKNOWLEDGMENT

The authors would like to thank D. Sheridan, IBM Microelectronics, Essex Junction, VT, D. Ahlgren, IBM Microelectronics, S. Subbanna, IBM Microelectronics, D. Herman, IBM Microelectronics, B. Meyerson, IBM Microelectronics, and the IBM SiGe team for their contributions. The wafers were fabricated at IBM Microelectronics, Essex Junction, VT.

REFERENCES

[1] D. L. Harame, D. C. Ahlgren, D. D. Coolbaugh, J. S. Dunn, G. Freeman, J. D. Gillis, R. A. Groves, F. N. Hendersen, R. A. Johnson, A. J. Joseph, S. Subbanna, A. M. Victor, K. M. Watson, C. S. Webster, and P. J. Zampardi, "Current status and future trends of SiGe BiCMOS technology," *IEEE Trans. Electron Devices*, vol. 48, pp. 2575–2594, Nov. 2001.

[2] L. S. Vempati, J. D. Cressler, J. A. Babcock, R. C. Jaeger, and D. L. Harame, "Low-frequency noise in UHV/CVD epitaxial Si and SiGe bipolar transistors," *IEEE J. Solid-State Circuits*, vol. 31, pp. 1458–1467, Oct. 1996.

[3] B. V. Haaren, M. Regis, O. Llopis, L. Escotte, A. Gruhle, C. Mahner, R. Plana, and J. Graffeuil, "Low-frequency noise properties of SiGe HBT's and application to ultra-low phase-noise oscillators," *IEEE Trans. Microwave Theory Tech.*, vol. 46, pp. 647–652, May 1998.

[4] J. Tang, G. Niu, Z. Jin, J. D. Cressler, S. Zhang, A. J. Joseph, and D. L. Harame, "Low-frequency noise figures-of-merit in RF SiGe RF technology," in *RFIC Symp. Tech. Dig.*, Seattle, WA, June 2002, pp. 179–182.

[5] L. K. J. Vandamme and G. Trefan, "Review of low-frequency noise in bipolar transistors over the last decade," in *Proc. IEEE Bipolar/BiCMOS Circuits and Technol. Meeting*, 2001, pp. 68–73.

[6] X. Wang, D. Wang, C. Masse, and P. Bacon, "Low phase noise SiGe voltage-controlled oscillators for wireless applications," *Microwave J.*, vol. 45, no. 2, pp. 84–99, Feb. 2002.

[7] S. P. Voinigescu, M. C. Maliepaard, J. L. Showell, G. E. Babcock, D. Marchesan, and M. Schroter, "A scalable high-frequency noise model for bipolar transistors with application to optimal transistor sizing for low-noise amplifier design," *IEEE J. Solid-State Circuits*, vol. 32, pp. 1430–1439, Sept. 1997.

[8] D. C. Ahlgren, M. Gilbert, D. Greenberg, J. Jeng, J. Malinowski, D. Nguyen-Ngoc, K. Schonenberg, K. Stein, R. Groves, K. Walter, G. Hueckel, D. Colavito, G. Freeman, D. Sunderland, D. L. Harame, and B. Meyerson, "Manufacturability demonstration of an integrated SiGe HBT technology for the analog and wireless marketplace," in *Int. Electron Devices Meeting Tech. Dig.*, 1996, pp. 859–862.

[9] G. Niu, S. Zhang, J. D. Cressler, A. J. Joseph, J. S. Fairbanks, L. E. Larson, C. S. Webster, W. E. Ansley, and D. L. Harame, "SiGe profile design tradeoffs for RF circuit applications," in *Int. Electron Devices Meeting Tech. Dig.*, 1999, pp. 573–576.

[10] ——, "Noise modeling and SiGe profile design tradeoffs for RF applications," *IEEE Trans. Electron Devices*, vol. 47, pp. 2037–2044, Nov. 2000.

[11] D. B. Leeson, "A simple model of feedback oscillator noise spectrum," *Proc. IEEE*, vol. 54, pp. 329–330, Feb. 1966.

[12] S. Zhang, G. Niu, J. D. Cressler, A. J. Joseph, G. Freeman, and D. L. Harame, "The effects of geometrical scaling on the frequency response and noise performance of SiGe HBTs," *IEEE Trans. Electron Devices*, vol. 49, pp. 429–435, Mar. 2002.

Jin Tang (S'02) was born in Sichuan, China, in November 1977. She received the B.S. degree in electrical engineering from the Huazhong University of Science and Technology, Wuhan, Hubei, China, in 2000, and is currently working toward the M.Sc. degree in electrical and computer engineering at Auburn University, Auburn, AL.

Her research is focused on the modeling and characterization of $1/f$ noise in SiGe HBT RF technology.

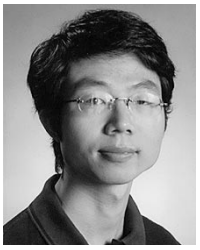

Guofu Niu (M'98–SM'02) was born in Henan, China, in December 1971. He received the B.S. (with honors), M.S., and Ph.D. degrees in electrical engineering from Fudan University, Shanghai, China, in 1992, 1994, and 1997, respectively.

From December 1995 to January 1997, he was a Research Assistant with the City University of Hong Kong, working on mixed-level device/circuit simulation and quantum effect programmable logic gates. From May 1997 to May 2000, he was a Post-Doctoral Researcher with Auburn University, Auburn, AL, where he focused on SiGe RF devices. In June 2000, he joined the faculty of Auburn University, where he is currently an Associate Professor of electrical and computer engineering. His research interests include SiGe devices and circuits, noise, single-event effects, SiC devices, low-temperature electronics, and technology computer-aided design (TCAD). He has authored or coauthored over 40 journal papers and over 40 conference papers related to his research. He is listed in *Who's Who in America*.

Dr. Niu served on the Program Committee of the 1997 Asia–South-Pacific Design Automation Conference (ASP-DAC) and currently serves on the Program Committee of the IEEE Bipolar/BiCMOS Circuits and Technology Meeting (BCTM). He has served as a reviewer for many journals, including IEEE ELECTRON DEVICE LETTERS, the IEEE TRANSACTIONS ON ELECTRON DEVICES, the IEEE TRANSACTIONS ON MICROWAVE THEORY AND TECHNIQUES, and IEEE MICROWAVE AND GUIDED WAVE LETTERS. He was the recipient of the T. D. Lee Physics Award in 1993 and 1994.

Zhenrong Jin (S'99) was born in Tianjin, China, in 1975. He received the B.S. and M.S. degrees in electrical engineering from Southeast University, Nanjing, China, in 1996 and 1999, respectively, and is currently working toward the Ph.D. degree in electrical and computer engineering at the Georgia Institute of Technology, Atlanta.

He has authored or coauthored several papers in the area of SiGe HBT devices. His current research interests include low-frequency noise in SiGe HBTs, low-noise RF circuits, and SiGe HBT device physics.

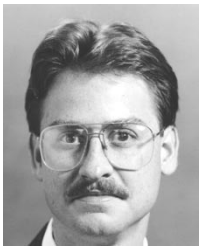

John. D. Cressler (S'86–A'91–SM'91–F'01) received the B.S. degree in physics from the Georgia Institute of Technology, Atlanta, GA, in 1984, and the M.S. and Ph.D. degrees in applied physics from Columbia University, New York, NY, in 1987 and 1990, respectively.

From 1984 to 1992. he was a member of the research staff at the IBM T. J. Watson Research Center, Yorktown Heights, NY, where he was involved with high-speed Si and SiGe bipolar devices and technology. In 1992, he join the faculty at Auburn University, Auburn, AL, where he remained until 2002. When he left Auburn University, he was the Philpott-Westpoint Stevens Distinguished Professor of Electrical and Computer Engineering and Director of the Alabama Microelectronics Science and Technology Center. In 2002, he joined the faculty of the Georgia Institute of Technology, where he is currently a Professor of electrical and computer engineering. His research interests include SiGe devices and technology, Si-based RF/microwave/millimeter-wave devices and circuits, radiation effects, noise and linearity, cryogenic electronics, SiC devices, reliability physics, two-dimensional (2-D)/three-dimensional (3-D) device-level simulation, and compact circuit modeling. He has authored or coauthored over 240 technical papers related to his research.

Dr. Cressler was an associate editor for the IEEE JOURNAL OF SOLID-STATE CIRCUITS (1998–2001), and served on the Technical Program Committees of the IEEE International Solid-State Circuits Conference (1992–1998, 1999–2001), the IEEE Bipolar/BiCMOS Circuits and Technology Meeting (1995–1999), the IEEE International Electron Devices Meeting (1996–1997), and the IEEE Nuclear and Space Radiation Effects Conference (1999–2000, 2002). He was the Technical Program chairman of the 1998 International Solid-State Circuits Conference (ISSCC). He currently serves on the Executive Steering Committee for the IEEE Topical Meeting on Silicon Monolithic Integrated Circuits in RF Systems, as international advisor for the IEEE European Workshop on Low-Temperature Electronics, and on the Technical Program Committee for the IEEE International SiGe Technology and Device Meeting. He was appointed an IEEE Electron Device Society Distinguished Lecturer in 1994, and was awarded the 1994 Office of Naval Research Young Investigator Award for his SiGe research program, the 1996 C. Holmes MacDonald National Outstanding Teacher Award by Eta Kappa Nu, the 1996 Auburn University Alumni Engineering Council Research Award, the 1998 Auburn University Birdsong Merit Teaching Award, the 1999 Auburn University Alumni Undergraduate Teaching Excellence Award, and an IEEE Third Millennium Medal in 2000.

Shiming Zhang, photograph and biography not available at time of publication.

Alvin J. Joseph (S'92–M'97) received the B.E. degree in electrical engineering from Bangalore University, Bangalore, India, in 1989, and the M.S. and Ph.D. degrees from Auburn University, Auburn, AL, in 1992 and 1997, respectively, both in electrical engineering. His doctoral research involved the study of physics, optimization, and modeling of cryogenically operated SiGe HBTs.

In 1997, he joined the SiGe Technology Development Group, IBM Microelectronics Division, Essex Junction, VT. He has been involved in various aspects of installing several SiGe BiCMOS technologies into production. He is currently the Process Integration Team Leader for the 0.18-μm SiGe BiCMOS technology. He has authored and coauthored several technical journal papers and conference publications related to SiGe HBTs.

Dr. Joseph was a member of the Device Physics Subcommittee for the IEEE Bipolar/BiCMOS Circuits and Technology Meeting (BCTM) (1997–2001).

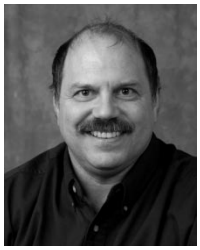

David L. Harame (S'77–M'83–SM'01) was born in Pocatello, ID, in 1948. He received the B.A. degree in zoology from the University of California at Berkeley, in 1971, the M.S. degree in zoology from Duke University, Durham, NC, 1973, the M.S. degree in electrical engineering from San Jose State University, San Jose, CA, in 1976, and the M.S. degree in materials science and the Ph.D. degree in electrical engineering from Stanford University, Stanford, CA, in 1984.

In 1984, he joined the Bipolar Technology Group, IBM T. J. Watson Research Center, Yorktown Heights, NY, where he was involved with the fabrication and modeling of silicon-based integrated circuits. His specific research interests at the IBM T. J. Watson Research Center included silicon and SiGe-channel FET transistors, n-p-n and p-n-p SiGe-based bipolar transistors, complementary bipolar technology, and BiCMOS technology for digital and analog and mixed-signal applications. In 1993, he joined the Semiconductor Research and Development Center (SRDC), Advanced Semiconductor Technology Center (ASTC), IBM, Hopewell Junction, NY, where he was responsible for the development of SiGe BiCMOS technology. He managed SiGe BiCMOS technology development at the ASTC through 1997. In 1998, he joined IBM's manufacturing organization, Essex Junction, VT, where he managed an SiGe technology group and installed the 0.5-μm SiGe BiCMOS process in the manufacturing line. In 1999, he rejoined the SRDC, while remaining in Essex Junction, V, T and co-managed the qualification of a 0.25-μm SiGe BiCMOS, as well as 0.18-μm SiGe BiCMOS and two derivative SiGe BiCMOS technologies. In May 2000, he assumed management of the SiGe BiCMOS RF Analog Models and Design Kits area. He currently manages the RF/analog and mixed signal technology, modeling, and design automation areas of the SRDC. He is a Distinguished Engineer of the IBM Corporation.

Dr. Harame is an Executive Committee member of the Bipolar/BiCMOS Circuits and Technology Meeting (BCTM) and a member of the Compact Model Council.